Supercoiling and Local Denaturation of Plasmids with a Minimalist DNA Model

ARTICLE *in* THE JOURNAL OF PHYSICAL CHEMISTRY B · OCTOBER 2008

Impact Factor: 3.3 · DOI: 10.1021/jp807085d · Source: PubMed

2 AUTHORS:

Fabio Trovato
Pennsylvania State University
13 PUBLICATIONS **70** CITATIONS
SEE PROFILE

Valentina Tozzini
Italian National Research Council
74 PUBLICATIONS **2,062** CITATIONS
SEE PROFILE

THE JOURNAL OF PHYSICAL CHEMISTRY B LETTERS

2008, *112,* 13197–13200
Published on Web 09/30/2008

Supercoiling and Local Denaturation of Plasmids with a Minimalist DNA Model

Fabio Trovato and Valentina Tozzini*

NEST CNR-INFM, Scuola Normale Superiore, Piazza dei Cavalieri 7, 56126 Pisa, Italy

Received: August 08, 2008; Revised Manuscript Received: September 04, 2008

We report molecular dynamics simulations of DNA nanocircles and submicrometer-sized plasmids with torsional stress. The multiple microseconds time scale is reached thanks to a new one-bead-per-nucleotide coarse-grained model that combines structural accuracy and predictive power, achieved by means of the accurate choice of the force field terms and their unbiased statistically based parametrization. The model is validated with experimental structural data and available all-atom simulations of DNA nanocircles. Besides reproducing the nanocircles' structures and behavior on the short time scale, our model is capable of exploring three orders of magnitude further in time and to sample more efficiently the configuration space, unraveling novel behaviors. We explored the microsecond dynamics of entire small plasmids and observed supercoiling and compaction in the overtwisted case. The stability of overtwisted nanocircles and plasmids is predicted up to macroscopic time scales. Conversely, in the undertwisted case, at physiological values of the superhelical density, after a metastable phase of supercoiling−compaction, we observe the formation and the complex dynamics of denaturation bubbles over a multiple microseconds time scale. Our results indicate that the torsional stress is involved in a delicate balance with the temperature to determine the denaturation equilibrium and regulate the transcription process.

Many biomolecular processes occur on the scale of microseconds to milliseconds and involve macromolecular aggregates sizing hundreds of nanometers to micrometers. Structural rearrangements occurring during the DNA condensation,[1] replication or repair,[2] fall in this class. These scales are still out of the capability of the all-atom force field (FF) based approaches, especially when one wants to address thermodynamic properties or structural transitions that require extensive simulations. In order to routinely reach the microscale in simulations, one can consider the coarse-grained (CG) models, which bring a gain of several orders of magnitude in the computational cost by grouping atoms in single interaction centers (beads) and consequently eliminating the internal fast degrees of freedom.[3,4] For the nucleic acids, several models with different levels of coarsening are available.[5−7] The one-bead (OB)-per-nucleotide representation is convenient in many respects. If the bead is placed on the P atom of the phosphate group, the model matches naturally with the cryo-electron microscopy structural data, often available for macromolecular aggregates, and is more suitable for the reconstruction of the all-atom structure.[6] At variance with coarser models, in the OB models, the internal variables suited for the description of structural transitions and denaturation are still explicitly present. Additionally, such a description naturally matches with available OB protein models, which makes this approach suitable for the simulation of DNA−protein complexes. In spite of these advantages, only a few OB nucleic acid models have gone beyond the harmonic bead−spring scheme,[8] due to the difficulty of merging accuracy, transferability, and predictive power.

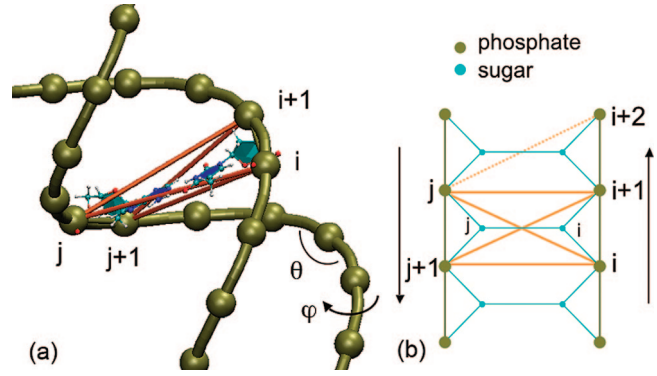

Figure 1. (a) Coarse-grained model of the DNA. The bead is placed on the P atom of the phosphate group. The base pairing bonds are shown in orange. The intrastrand internal variables are indicated. (b) A 2D scheme of the model. Arrows indicate the sense of the strand.

Recent OB models for the ribosome[9] and the nucleosome[10] have proven to accurately describe the slow modes of those macromolecular aggregates. However, retaining a certain amount of bias toward reference structures, those models suffer limited transferability.

In this paper, we report an unbiased OBCG model for DNA (Figure 1) that combines structural accuracy and predictive power. The FF is a sum of terms, $U = U_b + U_\theta + U_\varphi + U_{bp} + U_{nb}$, inspired by the standard all-atom FF. The first three are the intrastrand bonded terms (bond, bond angle, and dihedral) represented by harmonic functional forms. At variance with previous models,[9,10] the equilibrium parameters are based on the Boltzmann inversion[11] of the probability distributions obtained from a statistical set of experimental structures (details and parameters in the Supporting Information). This methodol-

* Corresponding author. Phone: +39-050-509433. Fax: +39-050-509417. E-mail: tozzini@nest.sns.it.

10.1021/jp807085d CCC: $40.75

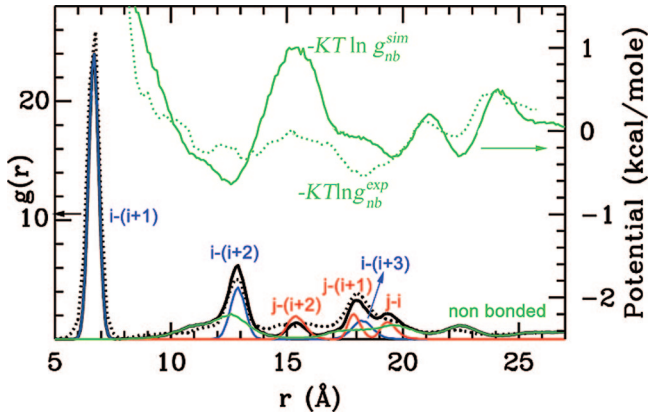

Figure 2. In the lower part: comparison between the radial distribution function from 200 ns of dynamics at 300 K of a 51-base-pair (bp) duplex (solid black line) and from a statistical set of X-ray structures linear DNA double strands (dotted black line). The intrastrand and interstrand components corresponding to bonded terms of the FF are shown in blue and red, respectively (indexed as in Figure 1). The nonbonded component is in green. The PMF, $V_{nb} = -kT \ln g_{nb}$, evaluated from the simulation (green solid line) and from the X-ray structures (green dotted line) are reported in the upper part (scale on the right).

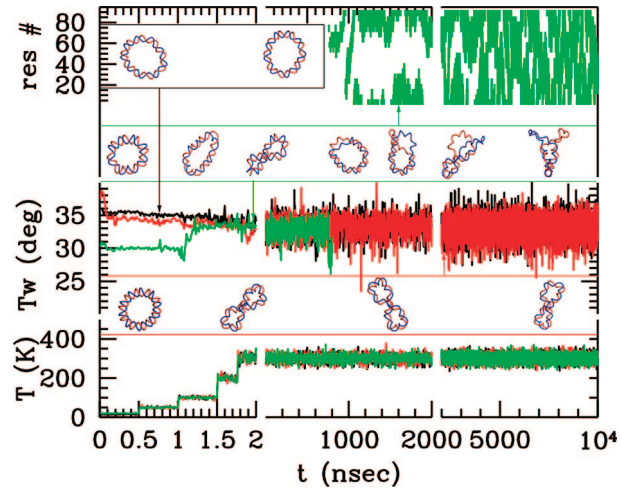

Figure 3. Simulations of heating and 300 K dynamics (Nose−Hoover thermostat) of a 92-bp DNA nanocircle. Black, relaxed ($L = 9$); red, overtwisted ($L = 10$, $\sigma = +0.11$); green, undertwisted ($L = 8$, $\sigma = -0.11$). The temperature and the average twist angle are reported. On the top, the dynamics of the bubble in the undertwisted case along the chain as a function of time is represented. At each time step, the residues where the bubble is present are colored in green. As the bubble forms, the average twist angle becomes meaningless and is no longer reported. The simulations are performed with the software DL_POLY.[17] Selected snapshots from the simulation are reported in the insets in the bottom (overtwisted, red box), in the center (undertwisted green box), and in the top (relaxed, black box). Starting structures are obtained with in-house-built software that generates a planar circular closed ring with a given number of base pairs per turn. A 1 μs long run needs approximately 8 h on a single processor.

ogy returns a parametrization that is independent from any specific reference structure.[3] The structural accuracy is mainly due to the use of innovative terms for the base pairing (U_{bp}) and the nonbonded interaction (U_{nb}). Figure 1 shows (in orange) the topology and geometry of U_{bp}, which is represented by three bonds for each base pair. This bonding topology accurately maintains the local geometry and torsion by including both the transversal force due to the hydrogen bonding and the longitudinal force due to base stacking. The functional form is a well-barrier-tail potential describing the hydrogen bond attraction and the electrostatic repulsion between phosphates. U_{nb} is a well-barrier-tail two-body potential as well, although in this case the well describes the hydrophobic interaction (details in the Supporting Information). These functional forms allow the DNA denaturation locating the transition of a linear double helix (51 bp) at 340 K (in agreement with experimental data). A detailed characterization of the phase diagram and of its dependence on the DNA sequence is the matter of a forthcoming paper.

We validate our model on experimental structural data and available all-atom simulations of DNA nanocircles. Figure 2 shows the comparison between the pair radial distribution function $g(r)$ obtained from our simulation and that obtained from a set of experimental structures (black solid and dotted lines, respectively). The matching of the peaks corresponding to the bonding terms (in blue and red) indicates that the strand geometry is accurately reproduced:[11,12] the values of the twist angles and of the rise agree with experimental data within a few percent (see the Supporting Information). The comparison between the nonbonded components is more conveniently shown through the corresponding potentials of mean force (PMF), derived from the $g(r)$ by Boltzmann inversion. The two main wells of the nonbonded PMF from our simulation (green solid line) correspond with those of its experimental counterpart (dotted green line), indicating that also the groove geometry is well reproduced (see also the Supporting Information). The small discrepancies are due to the presence of protein-bonded DNA in the experimental set that modifies the groove geometry with respect to the isolated DNA case considered in our simulations.

Our model is able to reproduce the behavior of DNA nanocircles with torsional stress observed in all-atom simulations.[13] Figure 3 reports heating and constant temperature simulations of a 92-bp nanocircle under different conditions of torsional stress, as measured by the superhelical density, $\sigma = (L - L_0)/L_0$, where L is the linking number (the number of times that the double helix winds around its axis) and L_0 is its value in the unstressed case.[14] All of the simulations start from planar structures with different average twist angles corresponding to different σ's. In the unstressed case (black line), the average twist (Tw) remains near to its equilibrium value, indicating that no global distortion occurs (the global geometry remains planar). In the overtwisted case (red), the value of Tw decreases almost immediately from the initially larger value to the equilibrium value. L is a topological invariant for closed circles that can be expressed as the sum of the global twist and of the writhe (Wr) measuring the contortion of the helix axis (see also the Supporting Information).[14] Thus, as Tw decreases, Wr increases, indicating the formation of the typical 8 shape. These results are in perfect agreement with those from the all-atom simulation of a nanocircle of the same size,[13] although in that case the transition is slower. This difference can be attributed in part to possibly different starting configurations and in part to the well-known acceleration effect in CG models, due to the intrinsic smoothening of the free energy landscape[4] (see also below). Assuming that the second effect is predominant, one obtains an estimate of about two orders of magnitude for the acceleration factor, which is in agreement with previous studies on HIV-1 protease.[3] Being aware that the relaxation times must be taken with great care in CG simulations, however, the unphysical acceleration of the dynamics is useful in this case, allowing a more efficient exploration of the configuration space. Indeed, we pushed our simulation on the multiple microsecond time scale (corresponding to approximately milliseconds if the acceleration correction is included) and did not observe significant changes in the global structure, although the crossing region of the "8" moves dynamically along the chain. This

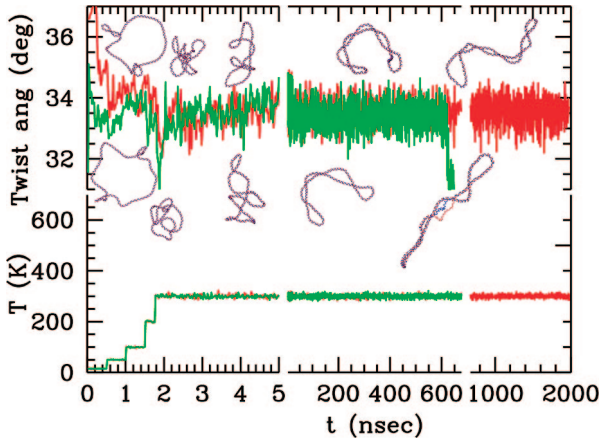

Figure 4. Simulations of heating and 300 K Langevin dynamics (damping constant $\gamma = 0.1$ ps^{-1}) of a 861-bp plasmid with torsional stress: red, overtwisted ($\sigma = +0.06$); green, undertwisted ($\sigma = -0.06$). The temperature and the average twist angle are reported. Selected snapshots from the simulation of undertwisted and overtwisted rings are reported below and above the twist angle plot, respectively. A 1 ns long run needs approximately 5 min on a single processor.

confirms the stability of the overtwisted nanocircles on the macroscopic time scales. A quantitative comparison of our structures with those obtained in the simulations of ref 13 is not possible, since no structure files are given therein. However, the qualitative comparison by means of the figures reported in ref 13 indicates a very close structural similarity of the CG structures with those of the all-atom simulations, both for the global shape and for the presence of kinks and defects, a further indication of the structural accuracy of our model.

In the undertwisted case (green), the metastable circular−planar configuration is maintained until the temperature reaches 100 K and then the transition to the compacted "8" shape occurs. Correspondingly, Tw rises to the equilibrium value, indicating the negative writhing. This configuration is maintained for ∼800 ns until a denaturation bubble opens (Figure 3, top graph), relaxing the torsional stress and reverting the global shape back to the circle. The bubble erratically moves along the circle maintaining the width of about 10−30 bp for about 1.5 μs and then gradually expands up to occupying almost half of the circle and distorting again the circle shape. Further bubble expansion seems to be hindered by the interwinding of the two strands. This behavior matches with recent experimental results[15] and is fully compatible with the "partial denaturation" reported in the all-atom simulations:[13] our simulation extends those results, illustrating the dynamics of the denaturation bubble, previously not accessible.

Our model allows us to consider systems as large as an entire small plasmid (861 bp, ∼0.3 μm circumference length) on the microsecond time scale (Figure 4). In plasmids, σ is found in a wide range,[16] although the physiological value $\sigma \approx -0.06$ is more generally maintained by topoisomerases.[1,2] This is the value we chose for the simulation (and the same absolute value for the positive case). As in the case of the nanoring, both in the undertwisted and overtwisted cases, the plasmid begins to writhe already in the heating phase. Starting from two opposite sides of the initially circular structure, an unstructured globule forms that subsequently develops into either positively or negatively writhed structures (movies in the Supporting Information). In this case, we used the Langevin dynamics[9] to partially account for the solvent effects. Correspondingly, the relaxation of the twist angle to the equilibrium value is slower than in the nanoring and displays several oscillations, also due to the larger conformational freedom. As in the case of the nanocircle, our simulation predicts stability of compacted positively writhed configurations in the overtwisted case, and the formation of a denaturation bubble in the undertwisted case. In spite of the smaller superhelical density, the bubble appears faster (within 1 ms) and has different dynamics with respect to the nanocircle. Instead of moving along the circle, it rapidly expands up to about 200 bp but remains trapped between two coils. Apparently, due to the more complexly writhed structure, the bubble is not able to relax the torsional stress enough to revert the structure to planar and then freely move along it.

As already pointed out, in DNA ring structures, the complete denaturation is forbidden due to the strand interwinding. However, our simulations show the formation of quite large denaturation bubbles. The metastability of the double helix already at relatively low σ is understood considering that DNA replication needs the strand separation: the replication-regulating enzymes can take advantage of this metastability for their action. At the same time, enzymes can stabilize the compact writhed form with a small change in the equilibrium, when necessary. Conversely, comparable levels of positive torsional stress produce compaction but not strand separation at 300 K. Positive torsional stress is often found in bacteria adapted to high temperatures.[16] Since the change of the temperature modifies the equilibrium value of the twist angle and thus the value of σ itself, it is likely that temperature and torsional stress levels interact in order to always maintain a level of (meta-) stability of the double helix proper for the strand separation to be easily regulated by enzymes as explained above.

In conclusion, we have reported and validated a novel CG model capable of high structural accuracy and predictive power. This model is capable of reproducing the results from all-atom simulations on DNA nanocircles. Being extremely computationally cheap, it allowed us to extend the exploration of the configuration space of nanocircles of several orders of magnitude with respect to all-atom simulations and to observe for the first time the dynamics of the denaturation bubbles. Additionally, we addressed an entire small plasmid, giving an accurate representation and predictions on a critical issue such as the dynamics of the DNA strand separation and its interplay with the torsional stress. Our results indicate that the undertwisting and the consequent metastability of the double helix have a main role in the regulation of the DNA transcription and replication that could be directly investigated by means of simulations of DNA in complex with regulating enzymes. This is within the potentiality of our model and is a natural application of it, together with the study of DNA compaction processes on the large scale.

Acknowledgment. We thank Joanna Trylska, Karine Woltz, and Fabio Beltram for useful discussions and Joanna Trylska also for having provided the Langevin dynamics module for DL_POLY. We acknowledge the allocation of computer resources from INFM "Progretto di calcolo Parallelo 2006."

Supporting Information Available: (1) The description of the FF, the Boltzmann inversion procedure, and details on the simulations analysis. (2) Selected simulation movies. This material is available free of charge via the Internet at http://pubs.acs.org.

References and Notes

(1) Bates, A. D.; Maxwell, A. *DNA topology*, 2nd ed.; Oxford University Press: Oxford, U.K., 2005.

(2) (a) Hatfield, G. W.; Benham, C. J. *Annu. Rev. Genet.* **2002**, *36*, 175–203. (b) Benham, C. J.; Bi, C. P. *J. Comput. Biol.* **2004**, *11*, 519–544. (c) Wang, J. C. *Biochim. Biophys. Acta* **1987**, *909*, 1–9.

(3) (a) Tozzini, V.; McCammon, J. A. *Chem. Phys. Lett.* **2005**, *413*, 123–128. (b) Tozzini, V.; Trylska, J.; Chang, C-E.; McCammon, J. A. *J. Struct. Biol.* **2007**, *157*, 606–615. (c) Trylska, J.; Tozzini, V.; McCammon, J. A. *Biophys. J.* **2005**, *89*, 1455–1463.

(4) (a) Tozzini, V. *Curr. Opin. Struct. Biol.* **2005**, *15*, 144–150. (b) Tozzini, V.; McCammon, J. A. One-Bead Coarse Grained Models for Proteins. In *Coarse-graining of condensed Phase and Biomolecular Systems*; Voth, G. A., Ed.; Taylor & Francis/CRC Press: London, 2008; Chapter 19.

(5) (a) Forrey, C.; Muthukumar, M. *J. Chem. Phys.* **2007**, *127*, 015102. (b) Arya, G.; Schlick, T. *Proc. Natl. Acad. Sci. U.S.A.* **2006**, *103*, 16236–16241. (c) Li, W.; Dou, S-X.; Xie, P.; Wang, P.-Y. *Phys. Rev. E* **2007**, *75*, 051915. (d) Korolev, N.; Lyubartsev, A. P.; Nordenskiöld, L. *Biophys. J.* **2006**, *90*, 4305–4316. (e) Stevens, M. J. *Biophys. J.* **2001**, *80*, 130–139.

(6) Mielke, S. P.; Grønbech-Jensen, N.; Krishnan, V. V.; Fink, W. H.; Benham, C. J. *J. Chem. Phys.* **2005**, *123*, 124911.

(7) (a) Tepper, H. L.; Voth, G. A. *J. Chem. Phys.* **2005**, *122*, 124906. (b) Drukker, K.; Wu, G.; Schatz, G. C. *J. Chem. Phys.* **2001**, *114*, 579–590. (c) Zhang, F.; Collins, M. A. *Phys. Rev. E* **1995**, *52*, 4217–4224. (d) Knotts, T. A., IV; Rathore, N.; Schwartz, D. C.; de Pablo, J. J. *J. Chem. Phys.* **2007**, *126*, 084901.

(8) Huertas, M. L.; Navarro, S.; Lopez Martinez, M. C.; Garcia de la Torre, J. *Biophys. J.* **1997**, *73*, 3142–3153.

(9) Trylska, J.; Tozzini, V.; McCammon, J. A. *Biophys. J.* **2005**, *89*, 1455–1463.

(10) (a) Voltz, K.; Wocjan, T.; Klenin, K.; Trylska, J.; Tozzini, V.; Kurkal, V.; Smith, J.; Langowski, J. *Biophys. J., Suppl. S* **2007**, 540A–540A. (b) Voltz, K.; Trylska, J.; Tozzini, V.; Kurkal-Siebert, V.; Langowski, J.; Smith, J. *J. Comput. Chem.* **2008**, *29*, 1429−1439.

(11) Reith, D.; Pütz, M.; Müller-Plathe, F. *J. Comput. Chem.* **2003**, *24*, 1624–1636.

(12) Zhou, J.; Thorpe, I. F.; Izvekov, S.; Voth, G. A. *Biophys. J.* **2007**, *92*, 4289–4303.

(13) (a) Harris, S. A.; Laughton, C. A.; Liverpool, T. B. *Nucl. Acids Res.* **2008**, *36*, 21–29. (b) Lankas, F.; Lavery, R.; Maddocks, J. H. *Structure* **2006**, *14*, 1527–1534.

(14) White, G. J.; Bauer, W. R. *Proc. Natl. Acad. Sci. U.S.A.* **1988**, *85*, 772–776.

(15) Du, Q.; Kotlyar, A.; Vologodskii, A. *Nucleic Acids Res.* **2008**, *36*, 1120–1128.

(16) Guipaud, O.; Marguet, E.; Noll, K. M.; DeLaTour, C. B.; Forterre, P. *Proc. Natl. Acad. Sci. U.S.A.* **1997**, *94*, 10606–10611.

(17) Smith, W.; Forester, T. R. *J. Mol. Graphics* **1996**, *14*, 136.

JP807085D